SUPPORTING INFORMATION

Molecular Mechanism of NDMA Formation from *N*,*N*-Dimethylsulfamide During Ozonation: Quantum Chemical Insights into a Bromide-Catalyzed Pathway

Daniela Trogolo[1], *Brijesh Kumar Mishra*[1†], *Michèle B. Heeb*[2], *Urs von Gunten*[2,3], *J. Samuel Arey*[1,3*]

[1] Environmental Chemistry Modeling Laboratory (LMCE), ENAC, Ecole Polytechnique Fédérale de Lausanne (EPFL), Lausanne, Switzerland

[2] Laboratory for Water Quality and Treatment (LTQE), ENAC, Ecole Polytechnique Fédérale de Lausanne (EPFL), Lausanne, Switzerland

[3] Eawag, Swiss Federal Institute of Aquatic Science and Technology, Dübendorf, Switzerland

[†] See present address (below).

Section S1. Standard State Terms Entering the $\Delta G_{aq,rxn}$ Calculation by eq 1

Following previous conventions,[1] here we consider that the free energies of gas phase species are given in the 1 atm gaseous standard state, denoted " ^{o} ", free energies of aqueous species are given in the "infinitely dilute" (i.e., not self-interacting) 1 M aqueous standard state, denoted " * ", and water is given in the pure liquid 55.56 M standard state, denoted " ^{l} ".

The Gibbs free energy of solvation, $\Delta G^*_{solv}(A_i)$, is defined as the free energy of transferring of a mole of A_i from the gas phase into aqueous solution, at infinitely dilute 1 M concentrations in both phases:

$$\begin{aligned}\Delta G^*_{solv}(A_i) &= G^*_{aq}(A_i) - G^*_{gas}(A_i) \\ &= G^*_{aq}(A_i) - \left(G^{o}_{gas}(A_i) + \Delta G^{o\rightarrow *}\right)\end{aligned} \quad \text{(S1)}$$

where $\Delta G^{o\rightarrow *}$ corresponds to the free energy change of compressing 1 mol of an ideal gas from 1 atm (0.04087 M) to 1 M at 298 K, or $-RTln(0.04087/1)$ = 1.89 kcal mol^{-1}.[2] The gas phase free energy at 1 M concentration, $G^*_{gas}(A_i)$, is obtained from the gas phase free energy at 1 atm, $G^{o}_{g,i}$, according to the relation $G^*_{gas}(A_i) = G^{o}_{gas}(A_i) + \Delta G^{o\rightarrow *}$.

For any reaction in aqueous phase, we can therefore write:

$$\begin{aligned}\Delta G^*_{aq,rxn} &= \textstyle\sum_i \nu_i \, G^*_{aq}(A_i) \\ &= \textstyle\sum_i \nu_i \left(G^*_{gas}(A_i) + \Delta G^*_{solv}(A_i)\right)\end{aligned} \quad \text{(S2)}$$

where ν_i is the stoichiometric coefficient of species A_i for the reaction step of interest.

Accordingly, for the reaction steps *f* and *j*, equation 1 (main text) would be written as:

$$\Delta G^*_{aq,rxn} = \textstyle\sum_i \nu_i \left(E_{gas,elec}(A_i) + G^{o}_{gas,therm}(A_i) + \Delta G^*_{SMD}(A_i) + \Delta G^{o\rightarrow *}\right) \quad \text{(S3)}$$

where $G^*_g(A_i) = E_{gas,elec}(A_i) + G^{o}_{gas,therm}(A_i) + \Delta G^{o\rightarrow *}$, and where $\Delta G^*_{solv}(A_i) = \Delta G^*_{SMD}(A_i)$. In practice, the term $\Delta G^*_{SMD}(A_i)$ is given by the energy difference of two single point calculations of the static solute: one with the SMD model and one without. The term $\sum_i \nu_i \, (\Delta G^{o\rightarrow *})$ corresponds to the $\Delta G_{Standard\ State}$ contribution to free energy of reaction, and thus eq S3 can be written as:

$$\Delta G^*_{aq,rxn} = \textstyle\sum_i \nu_i \left(E_{gas,elec}(A_i) + G^{o}_{gas,therm}(A_i) + \Delta G^*_{SMD}(A_i)\right) + \Delta G_{Standard\ State} \quad \text{(S4)}$$

The $\Delta G^*_{aq,rxn}$ value provided by eq S4 thus gives an equilibrium constant that is in the 1 M aqueous standard state.

For reaction steps *b* and *c*, which both generate H_2O as a product of the reaction, the free energy term of the generated water molecule is exceptionally converted to the pure liquid (55.56 M) standard state:

$$G_l(H_2O) = E_{gas,elec}(H_2O) + G^{o}_{gas,therm}(H_2O) + \Delta G^*_{SMD}(H_2O) + \Delta G^{o\rightarrow *} + \Delta G^{*\rightarrow l} \quad \text{(S5)}$$

where $\Delta G^{o\rightarrow *} + \Delta G^{*\rightarrow l}$ accounts for compressing a 1 atm (0.04087 M) ideal gas into 55.56 M liquid water at 298 K, or $-RTln(0.04087/55.56) = 4.27$ kcal mol^{-1}. Thus, for reaction steps *b* and *c*, $\Delta G^{*}_{aq,rxn}$ is still provided by eq S4 for non-H_2O solutes, but the free energy term for the H_2O solute, $G(H_2O)$, is substituted by eq S5. This gives an equilibrium constant in which the non-H_2O species are in the 1 M aqueous standard state and H_2O is in the pure liquid standard state. For these cases, the $\Delta G_{Standard\ State}$ contribution also includes the $\Delta G^{*\rightarrow l}$ term.

Section S2. Application of the Cluster-continuum Solvation Approach for $\Delta G_{aq,rxn}$ Calculations According to eq 2

For quantum chemistry simulation of ions in aqueous solution, specific solute-solvent interactions in the first solvation shell are typically quite important. Implicit solvent models are known to have difficulty capturing this effect. Bryantsev, Diallo, and Goddard have shown that a combined "cluster-continuum" solvation approach can lead to an improved description of equilibrium aqueous solvation free energies of ions.[3] According to the cluster-continuum method, the molecule of interest is treated as a geometry-optimized "cluster" of the solute together with a limited number of explicitly modeled water molecules. This cluster is further embedded in an implicit continuum dielectric field, taken to model the extant solvent. The previous work of Bryantsev et al.[3] explains how to obtain the Gibbs free energy of solvation for a molecule of interest (specifically, for ions), based on cluster-continuum calculations.

In the following section, we show how the cluster-continuum framework is extended to reactions. First we derive the expression for an intramolecular reaction (reaction step *k*), which is the simplest case. Then we evaluate the cases of step *o* and *p*, in which the solute dissociates into two product molecules, but the water cluster does not dissociate. Finally we consider a dissociation reaction (steps *l*, *m*), where the modeled water cluster itself becomes dissociated. The consequences of the cluster dissociation must be considered carefully in order obtain the correctly computed free energy of reaction in solution ($\Delta G^{*}_{aq,rxn}$) and also the correctly computed change in solvation free energy of the reaction ($\Delta\Delta G^{*}_{solv,rxn} = \Delta G^{*}_{aq,rxn} - \Delta G^{*}_{gas,rxn}$), according to the cluster-continuum framework. For ease of comparisons with the previous work, we adopt notation similar to that used by Bryantsev et al.[3]

According to the cluster-continuum framework presented by Bryantsev et al.,[3] the Gibbs free energy of solvation of molecule *A* may be computed by:

$$\Delta G^{*}_{solv}(A) =$$

$$\Delta G^{o,II}_{gas,bind,x}(A) + \Delta G^{*}_{SMD}(A(H_2O)_x) - \Delta G^{*}_{SMD}((H_2O)_x) - \Delta G^{o\rightarrow *} - RTln\left(\frac{[H_2O]}{x}\right) \quad \text{(S6)}$$

where $\Delta G^{*}_{solv}(A)$ is the free energy of solvation based on the infinitely dilute 1 M standard state. The term $\Delta G^{o,II}_{gas,bind,x}(A)$ is the free energy of binding between the gas phase molecule *A* and the gas phase cluster of water molecules, $(H_2O)_x$, following "cluster cycle II" in that paper:

$$\Delta G^{o,II}_{gas,bind,x}(A) = G^{o}_{gas}(A(H_2O)_x) - G^{o}_{gas}((H_2O)_x) - G^{o}_{gas}(A) \quad \text{(S7)}$$

In eqs S6 and S7, the lone species (*A*) indicates the unclustered molecule of interest, the species $A(H_2O)_x$ indicates a cluster of molecule *A* together with *x* explicit water molecules, and $[H_2O]$ represents the molar concentration of liquid water, 55.56 M. In eq S7, the terms $\Delta G^*_{SMD}(A(H_2O)_x)$ and $\Delta G^*_{SMD}((H_2O)_x)$ represent the free energies required to bring the clusters $A(H_2O)_x$ and $(H_2O)_x$ from gas phase into aqueous phase, as evaluated by the implicit solvent model (SMD, in the present work). We refer the reader to the previous paper[3] for complete explanation on the origins of the above equations.

First we evaluate $\Delta G^*_{aq,rxn}$ for an intramolecular rearrangement, which illustrates the cluster-continuum approach used for step *k* (Figure 1). Consider a reactant molecule *A* that is converted into product molecule *P*:

$$\Delta G^*_{aq,rxn} = G^*_{aq}(P) - G^*_{aq}(A) \tag{S8}$$

Following eqs S1 and S2, eq S8 can be re-written in terms of free energies of the gas phase species, G^{o}_{gas}, plus the aqueous solvation free energy, ΔG^*_{solv}, of each species:

$$\Delta G^*_{aq,rxn} = G^{o}_{gas}(P) + \Delta G^{o\rightarrow *} + \Delta G^*_{solv}(P) - G^{o}_{gas}(A) - \Delta G^{o\rightarrow *} - \Delta G^*_{solv}(A) \tag{S9}$$

It is worth noticing that in eq S9 the $\Delta G_{Standard\ State} = \sum_i \nu_i\ (\Delta G^{o\rightarrow *})$ term cancels to zero.

Upon substituting eqs S6 and S7 for the ΔG^*_{solv} terms in eq S9, several terms cancel to zero, and we arrive at:

$$\begin{aligned}\Delta G^*_{aq,rxn} = G^{o}_{gas}(P(H_2O)_x) - G^{o}_{gas}(A(H_2O)_x) + \Delta G^*_{SMD}(P(H_2O)_x) - \\ \Delta G^*_{SMD}(A(H_2O)_x)\end{aligned} \tag{S10}$$

where *x* corresponds to the number of explicit water molecules associated with the cluster containing each solute. By recognizing that $G^{o}_{gas} = E_{gas,elec} + G^{o}_{gas,therm}$, eq S10 can be re-written as:

$$\begin{aligned}\Delta G^*_{aq,rxn} = {} & E_{gas,elec}(P(H_2O)_x) - E_{gas,elec}(A(H_2O)_x) \\ & + G^{o}_{gas,therm}(P(H_2O)_x) - G^{o}_{gas,therm}(A(H_2O)_x) \\ & + \Delta G^*_{SMD}(P(H_2O)_x) - \Delta G^*_{SMD}(A(H_2O)_x)\end{aligned} \tag{S11}$$

Eq S11 is equivalent to eq 2 in the main text, where the $\Delta G_{cluster\ correction}$ term and $\Delta G_{standard\ state}$ term of eq 2 are both zero. Eq S11 eliminates the need to consider the unclustered gas phase product and reactant molecules. In other words, the reaction thermochemistry can be evaluated entirely by way of solvated clusters.

Eq S11 was applied to reaction step *k*. For the dissociation reaction steps *g*, *o*, and *p*, we also used eq S11, because in these cases the water cluster remains associated with a product fragment and does not break apart. However due to the fact that two product molecules are formed from the reaction steps *g*, *o*, and *p*, we had also to take into account an additional standard-state factor $(\Delta G^{o\rightarrow *})$.

Next we consider $\Delta G^*_{aq,rxn}$ for a reaction in which the cluster dissociates, which illustrates the cluster-continuum approach used for step *m* (Figure 1). In this case, reactant molecule *A* is converted into the product molecules P_1 and P_2:

$$\Delta G^*_{aq,rxn} = G^*_{aq}(P_1) + G^*_{aq}(P_2) - G^*_{aq}(A) \tag{S12}$$

We anticipate that the aqueously solvated species P_1, P_2, and *A* can be modeled as the clusters $P_1(H_2O)_y$, $P_2(H_2O)_z$, and $A(H_2O)_x$, where *y* is the number of explicit water molecules associated with the cluster containing P_1, *z* is the number of explicit water molecules in the cluster containing P_2, and *x* is the number of explicit water molecules in the cluster containing *A*. In order to maintain a balanced reaction, $x = z + y$.

Now, if we follow manipulations analogous to eqs S8-S11 above, fewer beneficent cancellations occur, and we find the expression:

$$\begin{aligned}\Delta G^*_{aq,rxn} = &\left(E_{gas,elec}\left(P_1(H_2O)_y\right) + E_{gas,elec}(P_2(H_2O)_z) - E_{gas,elec}(A(H_2O)_x)\right)\\ &+ \left(G^{o}_{gas,therm}\left(P_1(H_2O)_y\right) + G^{o}_{gas,therm}(P_2(H_2O)_z) - G^{o}_{gas,therm}(A(H_2O)_x)\right)\\ &+ \left(\Delta G^*_{SMD}\left(P_1(H_2O)_y\right) + \Delta G^*_{SMD}(P_2(H_2O)_z) - \Delta G^*_{SMD}(A(H_2O)_x)\right)\\ &+ \Delta G_{cluster\ correction}\end{aligned} \tag{S13}$$

where:

$$\begin{aligned}\Delta G_{cluster\ correction} = &-\left(E_{gas,elec}\left((H_2O)_y\right) + E_{gas,elec}((H_2O)_z) - E_{gas,elec}((H_2O)_x)\right)\\ &-\left(G^{o}_{gas,therm}\left((H_2O)_y\right) + G^{o}_{gas,therm}((H_2O)_z) - G^{o}_{gas,therm}((H_2O)_x)\right)\\ &-\left(\Delta G^*_{SMD}\left((H_2O)_y\right) + \Delta G^*_{SMD}((H_2O)_z) - \Delta G^*_{SMD}((H_2O)_x)\right)\\ &- RTln\left(\frac{x[H_2O]}{zy}\right)\end{aligned} \tag{S14}$$

Eq S13 is equivalent to eq 2 in the main text, where $\Delta G_{cluster\ correction}$ is given by eq S14, and the $\Delta G_{standard\ state}$ term (not shown) has canceled to zero.

Eq S13 is a convenient way to represent $\Delta G^*_{aq,rxn}$, because each major term is an intuitive result of straightforward simulations:

- The first three terms (first three lines of eq S13) are obtained by electronic, vibrational, and implicit solvent model calculations of the solvated clusters $P_1(H_2O)_y$, $P_2(H_2O)_z$, and $A(H_2O)_x$.
- The $\Delta G_{cluster\ correction}$ term (eq S14) is a less intuitive contribution that arises purely from the construction of the cluster-continuum framework. Collectively, the first three lines represent the free energy cost of dissociating the $(H_2O)_x$ water cluster into the two sub-

clusters, $(H_2O)_z$ and $(H_2O)_y$, all embedded in implicit solvent. This must be computed based on individually geometry-optimized water clusters having number *x*, *z*, and *y*. Conceptually, this term is viewed as a correction for the artifactual decrease in the number of inter-molecular contacts that result from the dissociation of the $A(H_2O)_x$ cluster into the two product clusters. Lastly, the term $-RTln\left(\frac{x[H_2O]}{zy}\right)$ comes from the standard state conversion of the water clusters into 55.56 M liquid water.[3]

- Eqs S13 and S14 eliminate the need to consider the unclustered gas phase product and reactant molecules. In other words, the reaction thermochemistry can be evaluated entirely by way of solvated clusters.

The magnitude of the $\Delta G_{cluster\ correction}$ term was 2.35 kcal mol^{-1} for the dissociation reaction *m*, according to eq S14. For this reaction, the explicit water clusters had populations of $x = 5$, $z = 3$, and $y = 2$. Geometries of the water clusters $(H_2O)_5$, $(H_2O)_3$, and $(H_2O)_2$ were optimized based on initial guess structures taken from Day et al.[4]

Finally, three product molecules were formed by the decomposition reaction *l*, but only two product species (Br^- and SO_2) were associated with water clusters. In this particular case, the $\Delta G^*_{aq,rxn}$ also contained the term $G^*_{aq}(P_3)$:

$$\Delta G^*_{aq,rxn} = G^*_{aq}(P_1) + G^*_{aq}(P_2) + G^*_{aq}(P_3) - G^*_{aq}(A) \tag{S15}$$

For the dissociation reaction *l*, we combined eqs S11 and S15 as follows:

$$\begin{aligned}\Delta G^*_{aq,rxn} = &\left(E_{gas,elec}\left(P_1(H_2O)_y\right) + E_{gas,elec}(P_2(H_2O)_z) - E_{gas,elec}(A(H_2O)_x)\right)\\ &+\left(G^o_{gas,therm}\left(P_1(H_2O)_y\right) + G^o_{gas,therm}(P_2(H_2O)_z) - G^o_{gas,therm}(A(H_2O)_x)\right)\\ &+\left(\Delta G^*_{SMD}\left(P_1(H_2O)_y\right) + \Delta G^*_{SMD}(P_2(H_2O)_z) - \Delta G^*_{SMD}(A(H_2O)_x)\right)\\ &+ (E_{gas,elec}(P_3) + G^o_{gas,therm}(P_3) + \Delta G^{o\rightarrow *} + \Delta G^*_{SMD}(P_3))\\ &+ \Delta G_{cluster\ correction}\end{aligned} \tag{S16}$$

where the $\Delta G_{cluster\ correction}$ is given by eq S14.

Section S3. Standard State Contributions to $\Delta G^{\ddagger}_{aq,rxn}$ According to eq 4

For the reaction steps *f* and *j*, we compute the free energies of activation by applying equation 4:

$$\begin{aligned}\Delta G^{\ddagger}_{aq,rxn} = &E^{\ddagger}_{gas,elec}(TS) + G^{\ddagger}_{gas,therm}(TS) + \Delta G^{\ddagger}_{SMD}(TS) - \textstyle\sum_i \Big(E_{gas,elec}(R_i) +\\ &G_{gas,therm}(R_i) + \Delta G_{SMD}(R_i)\Big) + \Delta G_{Standard\ State}\end{aligned} \tag{S17}$$

Where, R_i are the reactant species, *TS* is the transition state structure, and the $\Delta G_{Standard\ State}$ contribution to free energy of activation is defined as $\sum_i \nu_i\ (\Delta G^{o\rightarrow *})$ as for eq S4.

Finally, for reaction steps *b* and *g*, a cluster of water molecules was included in the simulations of both the reactant and the transition structure. For reaction *b*, the $\Delta G^{\ddagger}_{aq,rxn}$ was defined in a similar way as eq S11:

$$\begin{aligned}\Delta G^{\ddagger}_{aq,rxn} = {} & E^{\ddagger}_{gas,elec}(TS(H_2O)_x) - E_{gas,elec}(R_1(H_2O)_x) \\ & + G^{\ddagger}_{gas,therm}(TS(H_2O)_x) - G_{gas,therm}(R_1(H_2O)_x) \\ & + \Delta G^{\ddagger}_{SMD}(TS(H_2O)_x) - \Delta G^{*}_{SMD}(R_1(H_2O)_x) \\ & - (E_{gas,elec}(R_2) - G_{gas,therm}(R_2) - \Delta G^{o\rightarrow *} - \Delta G^{*}_{SMD}(R_2)) \end{aligned} \quad \text{(S18)}$$

The cluster of water does not dissociate in going from reactants to the transition state. For reaction step *b*, since there are two reactants and one transition state species, the $\Delta G_{Standard\ State}$ term is $-\Delta G^{o\rightarrow *}$.

Reaction step *g* has one reactant, and the $\Delta G^{\ddagger}_{aq,rxn}$ was defined as follows:

$$\begin{aligned}\Delta G^{\ddagger}_{aq,rxn} = {} & E^{\ddagger}_{gas,elec}(TS(H_2O)_x) - E_{gas,elec}(R_1(H_2O)_x) \\ & + G^{\ddagger}_{gas,therm}(TS(H_2O)_x) - G_{gas,therm}(R_1(H_2O)_x) \\ & + \Delta G^{\ddagger}_{SMD}(TS(H_2O)_x) - \Delta G^{*}_{SMD}(R_1(H_2O)_x) \end{aligned} \quad \text{(S19)}$$

For step *g*, the $\Delta G_{Standard\ State}$ term is cancelled out for reaction step *g*.

Section S4. Description of Minimum Energy Pathway Calculation (Relaxed Scan)

A relaxed scan describes the profile of the system electronic energy at several selected values of a chosen reaction coordinate. We used either the interatomic distance (bond length) or the angle between three bonded atoms as the reaction coordinate, depending on the reaction step. At each selected value of the reaction coordinate, a partially constrained geometry optimization of the system was conducted, maintaining a fixed value of the reaction coordinate while the remainder of the molecular system geometry is relaxed to an energy minimum. The resulting energy profile describes the minimum energy pathway along the reaction coordinate.

Section S5. Free Energy of the Proton in Aqueous Phase

The free energy of the proton in gas phase was assigned a value of $G(H^+)_{gas}$ = –6.28 kcal mol^{-1}.[5] This was converted from 1 atm to the 1 M standard state at 298 K by adding $\Delta G^{o\rightarrow *}$ = 1.89 kcal mol^{-1}. To this we added the free energy of solvation of the proton, $\Delta G(H^+)_{solv}$ = – 263.12 kcal mol^{-1}.[6] The resulting value of –267.51 kcal mol^{-1} was employed for $G(H^+)_{aq}$ in the 1 M aqueous

standard state and was used for computations of free energy of aqueous deprotonation reaction in eq 7. However the value for $G(H^+)_{aq}$ is cancelled out in the LFER used to estimate pK_a.

Section S6. Considerations on the validity of the quantum chemical modeling approach for aqueous reaction chemistry.

Comparison of theoretical and experimental reaction rate constants for selected reactions.

Reaction	Computed k ($M^{-1}s^{-1}$)	Experimental k ($M^{-1}s^{-1}$)
$HOBr + NH_3$	$10^{5\pm2.5}$	7.5×10^7 Ref. [7]
$HOBr + NH(CH_3)_2$	$10^{9\pm2.5}$	3.0×10^9 Ref. [7]
$O_3 + Br^-$	$10^{4\pm2.5}$	2.58×10^2 Ref. [8]

The theoretical rate constants for these three reactions were in agreement with the experimental estimates, to within expected errors of the modeling approach. This provides validation for the theoretical method applied to the related reactions *b* and *j*.

To further evaluate the appropriateness of our modeling approach, we also applied several other electronic structure methods to the free energy of reaction for step *b* (Table S2). The results obtained using other methods for geometry optimizations (B2PLYP, B2PLYPD, MP2, M06-L) are consistent with the values obtained with M05 geometries. Additionally, the reliable CCSD(T) wavefunction method confirms our energy results obtained by B2PLYPD. Finally, $\Delta G_{aq,rxn}$ results obtained with three explicit molecules of water are consistent with results obtained without explicit molecules of water. This suggests that the implicit solvent model (SMD) sufficiently accounts for the influence of directed solute-solvent interactions on the thermochemistry of this reaction.

In this study, we chose to optimize all geometries in gas phase. Geometry optimization and the vibrational analysis using implicit solvent models are often difficult to converge,[9] especially for transition state structures. For some reaction steps, we assumed that the solvent does not substantially affect the geometries of the involved species and the molecular mechanism. In those cases where the solvent is suspected to be directly involved in the reaction, we introduced explicitly modeled water molecules into the gas phase geometry optimizations.

Tarade et al.[10] used a similar approach to study the chlorination mechanism of organic amines by HOCl. In that work, structures were optimized in gas phase, and explicit molecules of water were included in the calculations of the transition structures. Implicit solvent calculations were then carried out on the gas phase micro-solvated clusters. Free energies of activation were computed with the B2PLYPD model chemistry. Tarade et al. also compared geometry optimizations and frequencies performed with an implicit solvent model to those obtained in gas phase. Use of the implicit solvent model was found to lead to very small changes in the geometries of the reactants and transition state structures. Thus the Tarade et al. study supports the assumption that gas phase geometries of microsolvated clusters were sufficient to describe transition state structures of the chlorination of amines by HOCl.

Section S7. Quantum chemical modeling of the activation free energy of reaction step *g*.

The reaction free energy of activation of step *g* was modeled with one explicit water molecule hydrogen-bonded to the electron-deficient proton of the NHBr fragment of Br-DMS. This explicit solvent cluster arrangement is justified as follows. According to NPA charges analysis, the transition state structure of reaction step *g* is characterized by two negatively-charged nitrogen atoms and a net neutral SO_2 leaving group. In this reaction mechanism, a bond between the two geminal nitrogen atoms can be formed by cleaving the SO_2 fragment. The extrusion of SO_2 group can only take place if the SO_2 group would gain electron density from the molecule. Thus, by associating one explicit molecule of water that can donate electron density to the proton of the NHBr fragment, the overall transition state structure is stabilized. We expect that specific interactions with the solvent would further stabilize the transition state only by way of increased transfer of electron density that would help to liberate the electron-deficient SO_2 group. However, aside from the proton of the NHBr fragment, no other hydrogen-bond donor groups are available on the molecule to accept electron density from solvent. Thus, the addition of more explicit water molecules is considered unlikely to influence substantially the reaction barrier.

Section S8. Reaction Steps *a, b, c,* and *d* in the Presence of HOCl. Chlorination Rates of DMS versus DMS^- and Speciation Equilibria of Cl-DMS / Cl-DMS^-.

Previous experimental work demonstrated that *N*,*N*-dimethylsulfide forms NDMA in the presence of HOCl and O_3, absent bromide.[11] This suggests that a rapid chlorination of *N*,*N*-dimethylsulfamide takes place, forming Cl-DMS / Cl-DMS^- (Figure 1, reactions *a*-*d*), analogous to the mechanism involving HOBr discussed in the main text. We did not conduct stopped-flow kinetic experiments with HOCl. Rate constants for halogenation by HOBr typically exceed those of HOCl by 2 to 3 orders of magnitude, for organic compounds.[12] By analogy to our results with HOBr, chlorination of DMS^- by HOCl (reaction pathway *c*) is expected to predominate over pathway *b*. The resulting Cl-DMS^- anion would become partly protonated at neutral pH, since the conjugate acid Cl-DMS has an estimated pK_a of 7.9 based on quantum chemical computations (main text). Based on these considerations, the expected predominating pathway for chlorination of *N*,*N*-dimethylsulfamide (steps *a*, *c*) parallels that of the bromination pathway.

Section S9. Reactions of Intermediates *B, C, D,* and *F* in the O_3 + HOCl System

When substituted with chlorine (X = Cl) instead of bromine, structure *B* undergoes a similar reaction branching, according to quantum chemical calculations. Again using the elongated N-S bond as a reaction coordinate, the chlorinated $B(H_2O)_5$ complex is found to have a low activation free energy of 2.5 kcal mol^{-1} for reaction step *o*, indicating that the corresponding reaction rate is very fast ($k_o \sim 10^{11\pm1.5}$ s^{-1}). However, unlike the situation with bromine, the chlorinated $B(H_2O)_5$ complex also experiences an apparently low activation free energy of 3.6 kcal mol^{-1} for the departure of the halide ion (reaction *m*) to produce intermediate *F*, corresponding to a near-thermally-controlled reaction rate ($k_m \sim 10^{10\pm2.5}$ s^{-1}). Intermediate *F* leads to the instantaneous formation of NDMA, as discussed below. Finally, based on relaxed scan calculations of the N-S-N angle, the chlorinated $B(H_2O)_5$ complex encounters a low free energy of activation of 4.2 kcal

mol^{-1} for the intramolecular rearrangement reaction *k*, indicating a reaction of $k_k \sim 10^{10\pm2.5}$ s^{-1}. This leads immediately to formation of NDMA. Step *k* is analogous to ClNO reaction with dimethylamine, which produces NDMA.[13] Thus the three reaction steps *o*, *m*, and *k* all exhibit very low reaction activation free energis, corresponding to fast first order reaction rates.

Analysis of reaction thermodynamics indicates that the three pathways (*o*, *m*, *k*) are near-neutral or favorable. Reactions *o* and are *m* approximately neutral, with $\Delta G_{aq,rxn}$ values of −1.4 and 2.1 kcal mol^{-1}, respectively. Reaction *k* is thermodynamically favorable, with estimated $\Delta G_{aq,rxn} = -4.0$ kcal mol^{-1}. However these decomposition reactions are interpreted as irreversible at the dilute concentrations of the products. Hence the back-reactions are considered unimportant.

In summary, O_3 reacts very rapidly with Cl-DMS$^-$ to form chlorinated intermediate *B*, which can readily decompose either via pathways that forms NDMA (steps *k*, *m*) or a pathway that does not form NDMA (step *o*). Analogous to the bromine-containing system, we are unable to resolve the differences in the rates of these three reaction branches, within the accuracy of the methods applied here. Thus we remain unable to explain the differences in yield of NDMA from DMS that have been observed previously in the O_3+bromide system versus the O_3+HOCl system. However our analysis demonstrates a fast pathway for NDMA formation from *N*,*N*-dimethylsulfamide in the presence of O_3 and HOCl, analogous to that in the O_3+bromide system.

Section S10. Intermediate *F* Leads to NDMA

Intermediate *F*, which is not a halogenated molecule, can rapidly form NDMA. Relaxed scan calculations were performed with the N-S-N angle as a reaction coordinate. IRC calculations confirmed that the transition state connected the reactants and products. The resulting SO_2 extrusion activation free energy of 3.1 kcal mol^{-1} (reaction *n*) leads to the formation of NDMA (Figure S4). This corresponds to a very fast rate constant of $k_n \sim 10^{10\pm2.5}$ s^{-1}. According to calculations, the SO_2 extrusion step *n* is very fast, exothermic, thermodynamically favored ($\Delta G_{aq,rxn} = -38.0$ kcal mol^{-1}), and effectively irreversible.

Section S11. Theoretical branching ratios for the decomposition of structures *B* and *C*.

Following the suggestion of a reviewer, we calculated the branching ratios for intermediates *B* and *C*, using the formula:

$$\beta^X{}_y = \frac{k_y}{\sum_{z=y}^{n} k_z} \tag{S20}$$

where β_y is the branching of reaction *y*, k_y is the rate constant of reaction *y* and $\sum_{z=y}^{n} k_z$ is the sum of all the other rate constants associated with the compound *X*. For structure *B*, the pathways *o*, *k*, and *l* were considered, whereas pathway *j* was excluded because it is irreversible. For structure *C*, we considered pathways *l*, *p*, and *k*.

The uncertainties of β_y were calculated as follows:

$$\beta^{X}{}_{y,upper\ bound} = \frac{k_y^{high}}{k_y^{high} + \sum_{z \neq y}^{n} k_z^{low}} \quad \text{(S21)}$$

$$\beta^{X}{}_{y,lower\ bound} = \frac{k_y^{low}}{k_y^{low} + \sum_{z \neq y}^{n} k_z^{high}} \quad \text{(S22)}$$

where k_y^{high} (k_y^{low}) is the rate constant calculated by adding (or subtracting) a factor of 3 kcal mol^{-1} to the free energy of activation.

Species	Reaction Step	β_y	$\beta^{X}{}_{y,upper\ bound}$	$\beta^{X}{}_{y,lower\ bound}$
B	*o*	0.7	0.99998	0.00009
	k	0.3	0.99990	0.00002
	m	10^{-7}	0.004	10^{-11}
C	*k*	10^{-6}	0.05	10^{-10}
	l	0.998	0.99999996	0.04
	p	0.001	0.96	10^{-9}

Figures and Tables

Figure S1.

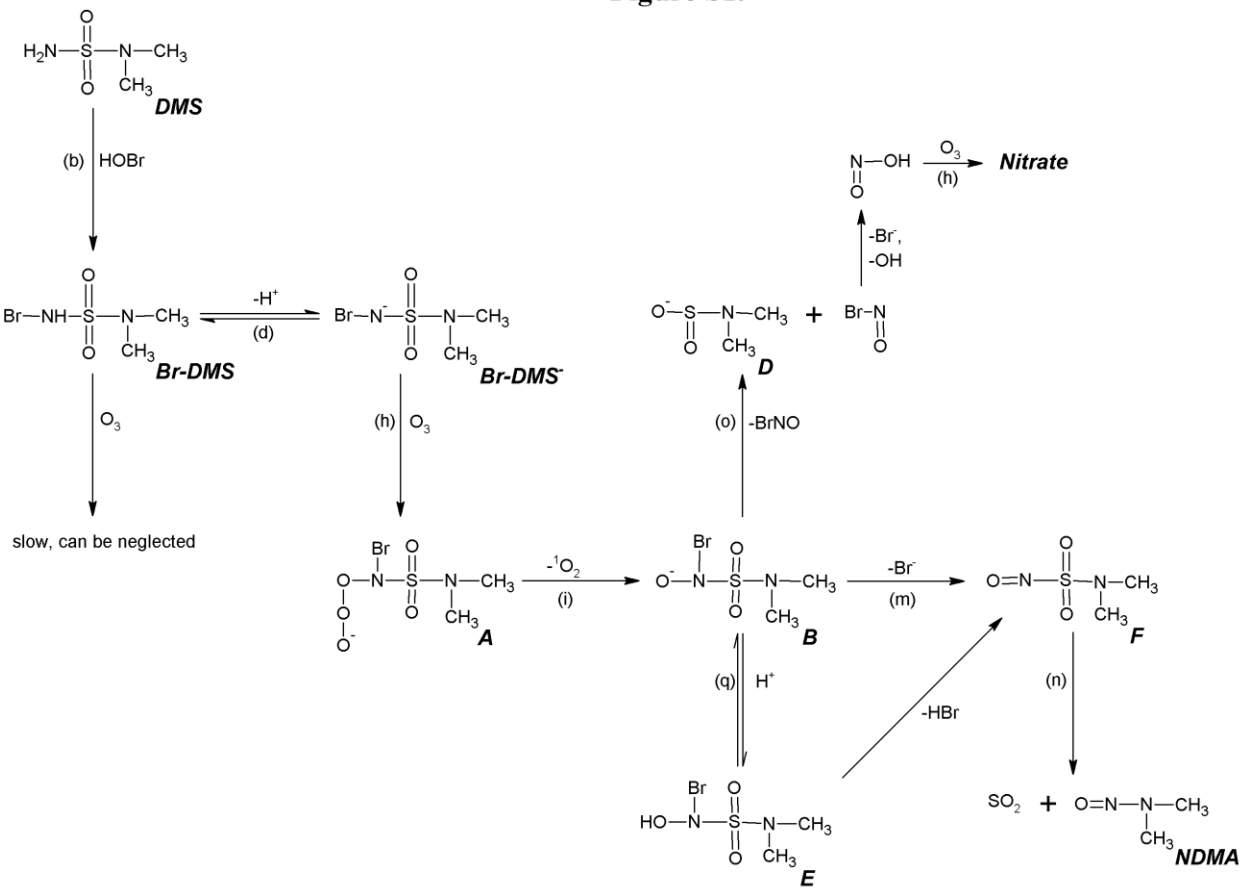

Figure S1. The previously proposed NDMA-formation pathway from *N*,*N*-dimethylsulfamide during ozonation of natural water.[11] The above figure is a based on "Scheme 2" in that work. However for clarity we have re-labeled the elementary reaction steps and intermediate structures according to Figure 1 of the present study.

Figure S2.

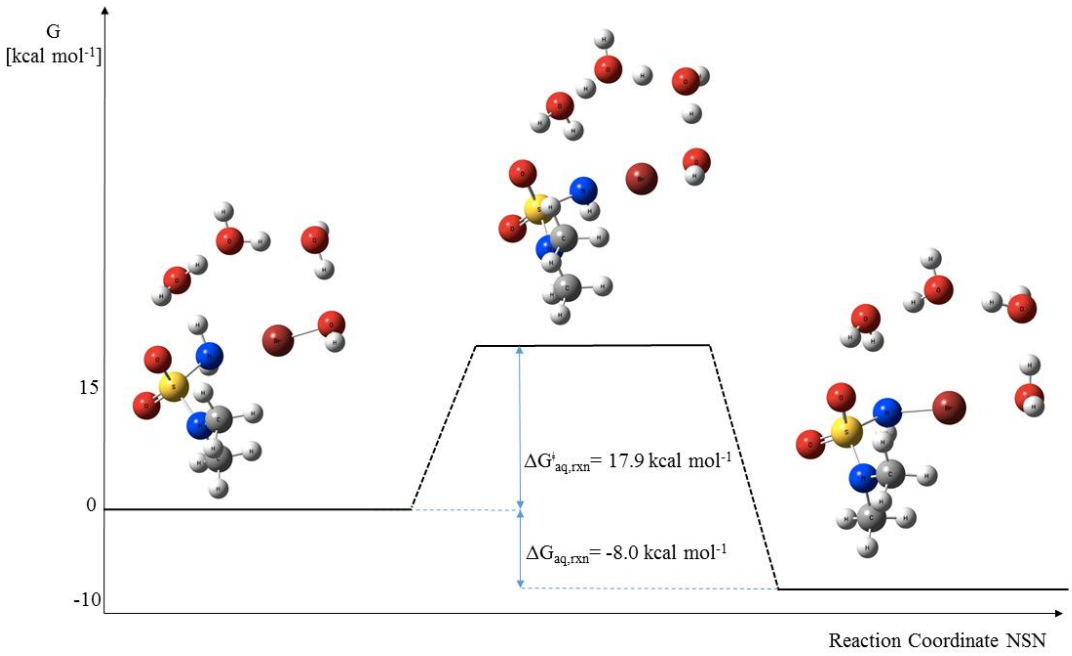

Figure S2. Bromination of neutral DMS by HOBr (reaction step *b*). According to quantum chemical calculations, the bromination reaction is facilitated by a proton shuttle involving three water molecules. Without the inclusion of explicit water molecules in the simulation, the computed reaction activation free energy is raised by >40 kcal mol^{-1}, which would correspond to an infeasible mechanism.

Figure S3.

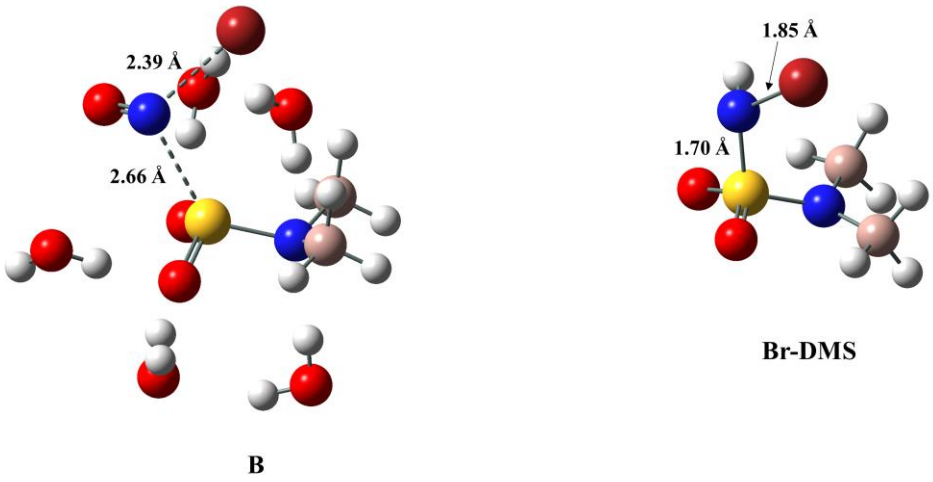

Figure S3. The anionic intermediate structure *B* (left) and Br-DMS (right), according to M05/aug-cc-pVTZ geometry optimizations in gas phase. The N-Br bond (2.39 Å) and N-S bond (2.66 Å) in structure *B* are both significantly elongated compared to the same bonds in Br-DMS, consistent with bond weakening. In the optimized $B(H_2O)_5$ cluster, explicit water molecules donate hydrogen-bonds to the two sulfonyl oxygen atoms, to the dimethyl-substituted N atom, and to the Br atom. This arrangement is intuitively reasonable: according to NPA calculations, these four atoms of structure *B* all bear substantial partial negative charge (Figure 2), indicative of excess electron density that is available to participate in hydrogen-bonding with the solvent.

Figure S4.

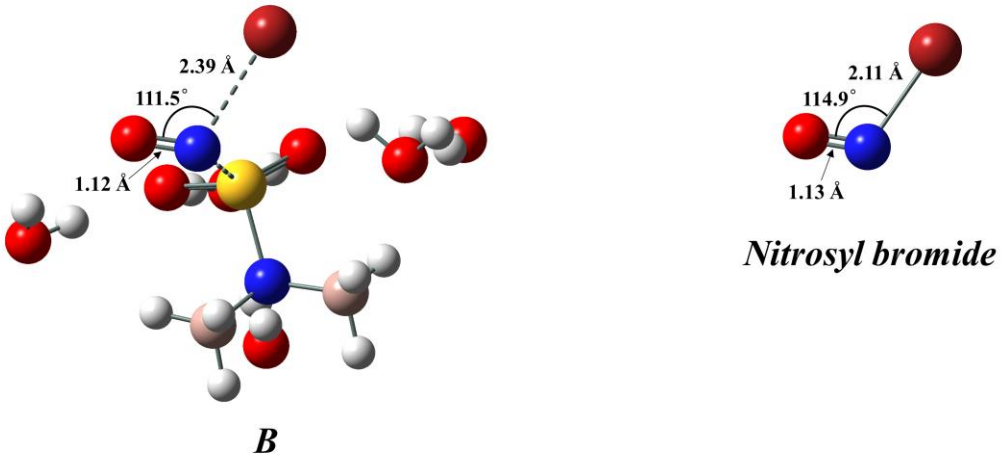

Figure S4. Geometric parameters of the BrNO fragment in intermediate structure *B* (left) are compared with those observed for nitrosyl bromide (right), based on M05/aVTZ geometry optimization in gas phase. The computed N=O bond length and Br-N=O angle in structure *B* are comparable to those of nitrosyl bromide. The N-Br bond of structure *B* is lengthened compared to nitrosyl bromide, consistent with bond weakening.

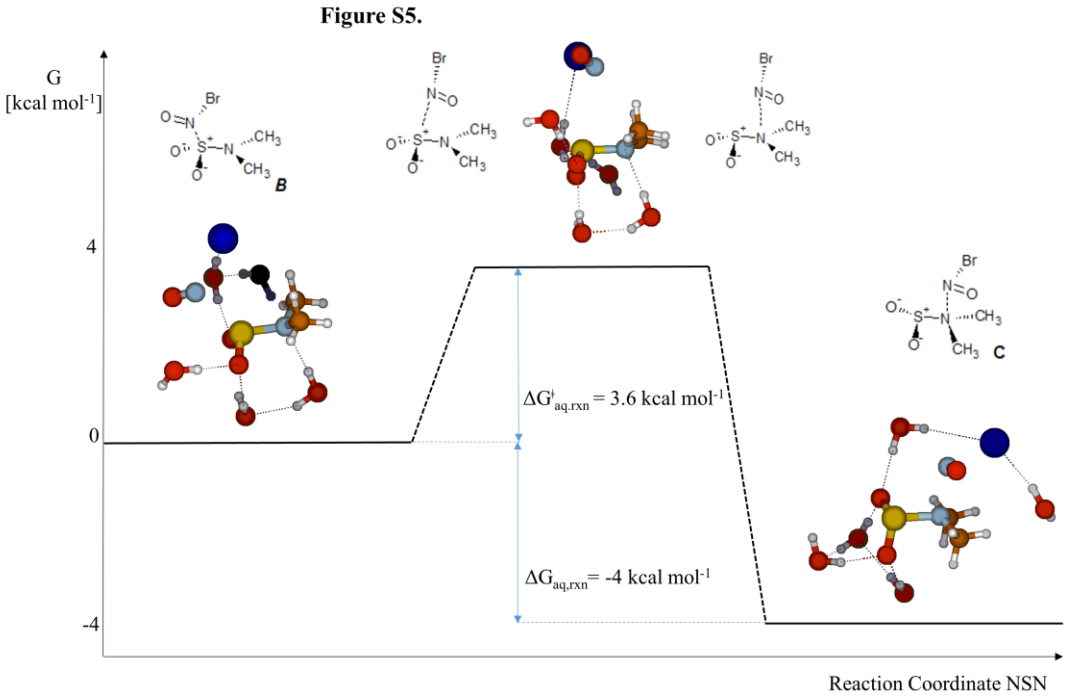

Figure S5. Schematic of reaction step *k*: the intermediate structure *B* (left), intermediate structure *C* (right), and the intervening activated structure (middle). Explicit water molecules included in the simulation are also shown. Lewis structures are proposed (top) based on NPA charge results.

Figure S6.

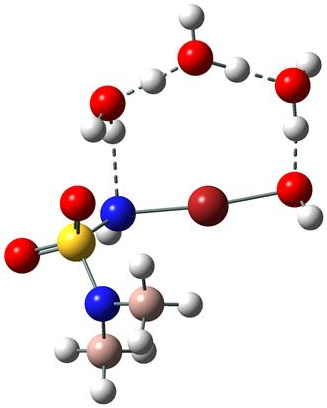

Step *b* Transition State Structure

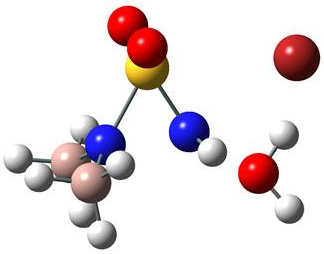

Step *g* Transition State Structure

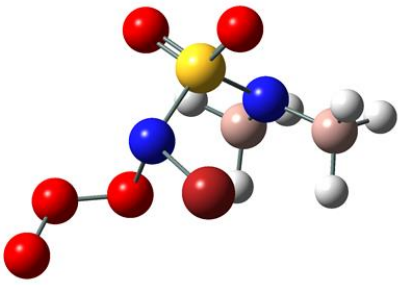

Step *j* Transition State Structure

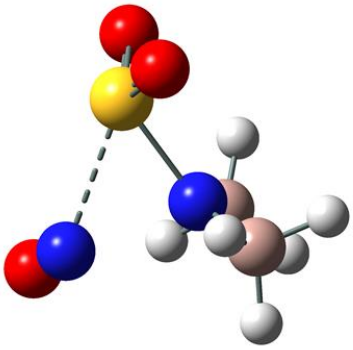

Step *n* Transition State Structure

Figure S6. Transition State Structures of reaction steps *b*, *g*, *j*, and *n*. These structures were obtained from a transition state search with the M05/aug-cc-pVTZ model chemistry in gas phase.

Table S1. Evaluation of M05, M06, B2PLYP, and B2PLYPD for the Error per bond in Total Atomization Energies (T.A.E.) of O_3, NO, N_2O, HNO, SO_2, and Br_2, in kcal mol^{-1}.

	Benchmark	M05/aug-cc-pVTZ		M06/aug-cc-pVTZ		B2PLYP/aug-cc-pVTZ		B2PLYPD/ aug-cc-pVTZ	
Molecule	W4 T.A.E.[a]	T.A.E.	Error per bond[b]	T.A.E.	Error per bond	T.A.E.	Error per bond	T.A.E.	Error per bond
O_3	147.35	137.19	5.08	137.40	4.98	145.27	1.04	145.29	1.03
NO	152.30	149.35	2.95	148.92	3.38	153.42	–1.12	153.42	–1.12
N_2O	269.63	276.24	–3.30	273.87	–2.12	274.58	–2.48	274.62	–2.49
HNO	205.45	200.49	2.48	201.78	1.84	203.67	0.89	203.69	0.88
SO_2	259.61	243.23	8.19	246.84	6.38	245.24	7.19	245.31	7.15
Br_2	52.82	45.30	7.52	49.71	3.11	49.45	3.37	49.46	3.36
MUE per bond[c]			3.82		2.93		1.48		1.47

[a] The W4 benchmark estimate of the molecular Total Atomization Energy at 0 K was taken from Karton et al. 2006, excluding zero point vibrational energy, core-valence correlation correction, scalar relativistic correction, spin-orbit coupling, and diagonalized Born-Oppenheimer correction. [b] Error per bond = (Benchmark T.A.E. – DFT T.A.E.) / (Total number of atoms – 1). [c] "Mean unsigned error" (MUE) is the average of the unsigned error per bond over the four molecules in the data set, in kcal mol^{-1}.

Table S2. Complete List of Computed Gibbs Free Energies of Reaction ($\Delta G_{aq,rxn}$) for Elementary Steps of the NDMA Formation Pathway

Reaction step[a]	Number of explicit waters included	Geometry Optimization Method[b]	$E_{gas,elec}$ Method[c]	$G_{gas,therm}$ Method[d]	ΔG_{SMD} Method[e]	Estimated Total $\Delta G_{aq,rxn}$ (kcal mol^{-1})	
						X^f = Br	X^f = Cl
b	3	M05	M05	M05	SMD/M05	–0.8	–6.6
b	3	M05	B2PLYPD	M05	SMD/M05	–8.0	–11.2
b	0	B2PLYP	B2PLYP	M05	SMD/M05	–6.9	–10.0
b	0	B2PLYPD	B2PLYPD	M05	SMD/M05	–7.8	–10.6
b	0	MP2	MP2	M05	SMD/M05	–11.4	–13.9
b	0	MP2	CCSD(T)	M05	SMD/M05	–9.3	–10.7
b	0	M05	M05	M05	SMD/M05	–6.2	–12.0
b	0	M05	B2PLYPD	M05	SMD/M05	–7.8	–11.0
b	0	M06-L	M06-L	M06-L	SMD/M06-L	–7.1	-
b	0	M06-L	B2PLYPD	M06-L	SMD/M06-L	–8.6	-
c	0	M05	M05	M05	SMD/M05	–15.4	–22.3
c	0	M05	B2PLYPD	M05	SMD/M05	–17.9	–21.5
f	0	M05	M05	M05	SMD/M05	3.7	
f	0	M05	B2PLYPD	M05	SMD/M05	1.9	
g	1	M05	M05	M05	SMD/M05	–12.3	-
g	1	M05	B2PLYPD	M05	SMD/M05	–20.1	-
j	0	M05	M05	M05	SMD/M05	–27.4	–33.0
j	0	M05	B2PLYPD	M05	SMD/M05	–30.7	–34.2
k	5	M05	M05	M05	SMD/M05	0.3	0.0
k	5	M05	B2PLYPD	M05	SMD/M05	–4.0	–4.0
l	5	M05	M05	M05	SMD/M05	–36.0	–36.4
l	5	M05	B2PLYPD	M05	SMD/M05	–26.2	–31.3
m	5	M05	M05	M05	SMD/M05	–0.3	–3.7
m	5	M05	B2PLYPD	M05	SMD/M05	6.2	2.1
n	0	M05	M05	M05	SMD/M05	–34.3	

n	0	M05	B2PLYPD	M05	SMD/M05	–34.6	
o	5	M05	M05	M05	SMD/M05	–6.4	–4.0
o	5	M05	B2PLYPD	M05	SMD/M05	–2.8	–1.4
p	5	M05	M05	M05	SMD/M05	–6.6	–4.1
p	5	M05	B2PLYPD	M05	SMD/M05	1.2	2.6

[a] Elementary reaction step as depicted in Figure 1 (main text). [b] Model chemistry used to optimize the molecular geometries to energetic minima, for the purpose of computed $\Delta E_{gas,elec}$ estimates. The aug-cc-pVTZ basis set was used for all geometry optimizations. [c] Model chemistry employed to compute the electronic energy of the reaction, at fixed nuclear coordinates in gas phase. The aug-cc-pVTZ basis set was used for all computed $\Delta E_{gas,elec}$ estimates, except CCSD(T), for which an aug-cc-pV{D,T}Z basis set extrapolation was applied. [d] Model chemistry used to compute the gas phase thermal contributions (vibrations, rotations, and translation) to the Gibbs Free Energy of reaction, with a consistently optimized geometry. The aug-cc-pVTZ basis set was used for all $\Delta G_{gas,therm}$ computations. [e] Solvation model and model chemistry employed to compute the change in Gibbs Free Energy of aqueous solvation for the reaction. The aug-cc-pVTZ or cc-pVTZ basis set was used. [f] Results are shown for both the O_3+bromide-catalyzed pathway (X = Br) and the O_3+HOCl system pathway (X=Cl).

Table S3. Complete List of Computed Activation Free Energies ($\Delta G^{\ddagger}_{aq,rxn}$) for Elementary Reaction Steps of the NDMA Formation Pathway

Reaction step[a]	Number of explicit waters included	Relaxed Scan Method[b]	$\Delta E^{\ddagger}_{gas,elec}$ Method[c]	$\Delta G^{\ddagger}_{gas,therm}$ Method[d]	$\Delta\Delta G^{\ddagger}_{SMD}$ Method[e]	Estimated Total $\Delta G^{\ddagger}_{aq,rxn}$ (kcal mol^{-1})	
						X^f = Br	X^f = Cl
b	3	M05	M05	M05	SMD/M05	15.6	-
b	3	M05	B2PLYPD	M05	SMD/M05	17.9	-
g	0	M05	M05	M05	SMD/M05	43.2	-
g	0	M05	B2PLYPD	M05	SMD/M05	36.4	-
g	1	M05	M05	M05	SMD/M05	39.4	-
g	1	M05	B2PLYPD	M05	SMD/M05	33.9	-
j	0	M05	M05	M05	SMD/M05	13.4	12.7
j	0	M05	B2PLYPD	M05	SMD/M05	10.6	10.5
k	5	M05	M05	-	SMD/M05	2.0	3.7
k	5	M05	B2PLYPD	-	SMD/M05	3.6	4.2
l	5	M05	M05	-	SMD/M05	<1.0	<1.0
m	5	M05	M05	-	SMD/M05	6.3	0.2
m	5	M05	B2PLYPD	-	SMD/M05	122	3.6
n	0	M05	M05	M05	SMD/M05	10.0	
n	0	M05	B2PLYPD	M05	SMD/M05	3.1	
o	5	M05	M05	-	SMD/M05	2.6	2.3
o	5	M05	B2PLYPD	-	SMD/M05	3.0	2.5
p	5	M05	M05	-	SMD/M05	1.4	5.4
p	5	M05	B2PLYPD	-	SMD/M05	5.1	11.4

[a] Elementary reaction step as depicted in Figure 1. [b] Model chemistry employed to perform relaxed scan computations, for the purpose of $\Delta E^{\ddagger}_{gas,elec}$ estimates. The aug-cc-pVTZ basis set was used throughout. [c] Model chemistry employed to compute the electronic energy of the reaction, at fixed nuclear coordinates in gas phase. The aug-cc-pVTZ basis set was used for all $\Delta E^{\ddagger}_{gas,elec}$ estimates. [d] Model chemistry used to compute the transition state search (where this was conducted) and subsequent frequency calculations. $\Delta G^{\ddagger}_{gas,therm}$ includes gas phase thermal contributions (vibrations, rotations, and

translation) to the Gibbs Free Energy of the transition state. The aug-cc-pVTZ basis set was used throughout. For some solvated clusters, the $\Delta G^{\ddagger}_{gas,therm}$ contribution was not computed, and these entries are left blank (see main text). [e] Solvation model and model chemistry employed to compute the change in Gibbs Free Energy of aqueous solvation upon going from reactant structure to the transition state structure. The aug-cc-pVTZ basis set was used. [f] Results are shown for both the O_3+bromide-catalyzed pathway (X = Br) and the O_3+HOCl system pathway (X=Cl).

Table S4. Experimental pK_a Data For 4 Neutral Nitrogen Acids and Quantum Chemical LFER pK_a Estimates for DMS, BrDMS, ClDMS

	Experimental pK_a value	Uncorrected[a] (raw) quantum chemical pK_a^{uncorr}	Quantum-chemical LFER pK_a estimate
Known pK_a data			
$CF_3SO_2NH_2/NH^-$	6.3[14]	8.59	5.0
$H_2NSO_2NH_2/NH^-$	10.4[15]	16.90	9.7
HN_3/N_3^-	4.72[14]	10.63	6.2
CH_3CONH_2/NH^-	15.1[14]	27.64	15.7
Estimated pK_a data			
DMS/DMS^-	10.4[b]	18.04	10.3
$BrDMS/BrDMS^-$	-	15.63	9.0
$ClDMS/ClDMS^-$	-	13.76	7.9

[a] Computed according to eq 7 in the main text. [b] Based on stopped-flow results and eq 8.

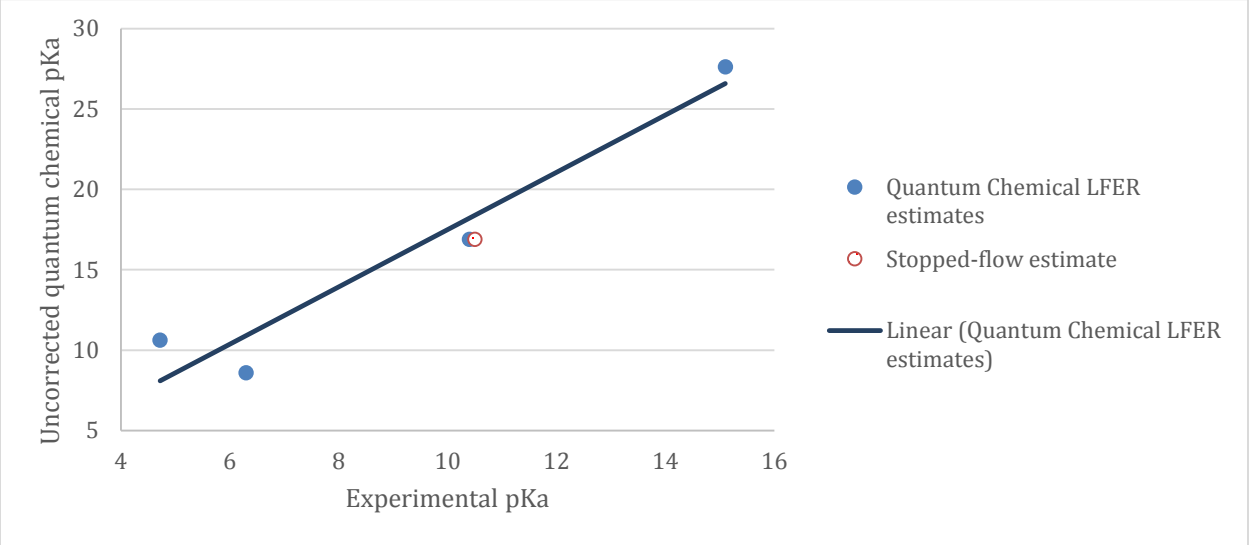

Figure S7. Graph showing the correlation between the experimental pK_a values and the uncorrected quantum chemical pK_a^{uncorr} results for hydrazoic acid, sulfamide, acetamide, and trifluoromethanesulfamide. The stopped-flow estimate of the pK_a value for DMS is the one indicated with the open red circle.

References

(1) Ben-Naim, A. *Solvation Thermodynamics*; Plenum Press, New York, 1987; p. 246.

(2) Kelly, C. P.; Cramer, C. J.; Truhlar, D. G. SM6 : A Density Functional Theory Continuum Solvation Model for Calculating Aqueous Solvation Free Energies of Neutrals, Ions, and Solute - Water Clusters. *J. Chem. Theory Comput.* **2005**, *1*, 1133–1152.

(3) Bryantsev, V. S.; Diallo, M. S.; Goddard III, W. A. Calculation of Solvation Free Energies of Charged Solutes Using Mixed Cluster/continuum Models. *J. Phys. Chem. B* **2008**, *112*, 9709–9719.

(4) Day, M. B.; Kirschner, K. N.; Shields, G. C. Global Search for Minimum Energy (H2O)n Clusters, n = 3-5. *J. Phys. Chem. A* **2005**, *109*, 6773–6778.

(5) Liptak, M. D.; Shields, G. C. Accurate pKa Calculations for Carboxylic Acids Using Complete Basis Set and Gaussian-n Models Combined with CPCM Continuum Solvation Methods. *J. Am. Chem. Soc.* **2001**, *123*, 7314–7319.

(6) Isse, A. A.; Gennaro, A. Absolute Potential of the Standard Hydrogen Electrode and the Problem of Interconversion of Potentials in Different Solvents. *J. Phys. Chem. B* **2010**, *114*, 7894–7899.

(7) Wajon, J. E.; Morris, J. C. Rates of Formation of N-Bromo Amines in Aqueous Solution. *J. Inorg. Chem.* **1982**, 4258–4263.

(8) von Sonntag, C.; von Gunten, U. *Chemistry of Ozone in Water and Wastewater Treatment: From Basic Principles to Applications*; IWA Publishing, 2012; p. 302.

(9) Liu, Y. D.; Selbes, M.; Zeng, C.; Zhong, R.; Karanfil, T. Formation Mechanism of NDMA from Ranitidine, Trimethylamine, and Other Tertiary Amines during Chloramination: A Computational Study. *Environ. Sci. Technol.* **2014**.

(10) Tarade, T.; Vrček, V. Reactivity of amines with hypochlorous acid: Computational study of steric, electronic, and medium effects. *Int. J. Quantum Chem.* **2013**, *113*, 881–890.

(11) von Gunten, U.; Salhi, E.; Schmidt, C. K.; Arnold, W. A. Kinetics and Mechanisms of N-Nitrosodimethylamine Formation upon Ozonation of Waters: Bromide Catalysis. *Environ. Sci. Technol.* **2010**, *44*, 5762–5768.

(12) Heeb, M. B.; Criquet, J.; Zimmermann-Steffens, S. G.; von Gunten, U. Oxidative treatment of bromide-containing waters: Formation of bromine and its reactions with inorganic and organic compounds - A critical review. *Water Res.* **2014**, *48*, 15–42.

(13) Fridman, A. L.; Mukhametshin, F. M.; Novikov, S. S. Advances in the Chemistry of Aliphatic N-Nitrosamines. *Russ. Chem. Rev.* **1971**, *40*, 34–50.

(14) Bordwell, G. Equilibrium Acidities in Dimethyl Sulfoxide Solution. *Acc. Chem. Res* **1988**, *21*, 456–463.

(15) Hannigan, T. J.; Spillane, W. J. Basicity of Nitrogen-Sulphur(VI) Compounds. Part 4.1 Ionization of Di- and Tri-substituted Sulphamides. *J. Chem. Soc. Perkin Trans. II* **1982**, 851–855.